

UCLA

UCLA Previously Published Works

Title

Aldehyde Dehydrogenase Activity Enriches for Proximal Airway Basal Stem Cells and Promotes Their Proliferation

Permalink

<https://escholarship.org/uc/item/0rs2m2br>

Journal

Stem Cells and Development, 23(6)

ISSN

1547-3287

Authors

Hegab, Ahmed E
Ha, Vi Luan
Bisht, Bharti
[et al.](#)

Publication Date

2014-03-15

DOI

10.1089/scd.2013.0295

Peer reviewed

Aldehyde Dehydrogenase Activity Enriches for Proximal Airway Basal Stem Cells and Promotes Their Proliferation

Ahmed E. Hegab,^{1,*} Vi Luan Ha,¹ Bharti Bisht,¹ Daphne O. Darmawan,¹ Aik T. Ooi,¹ Kelvin Xi Zhang,² Manash K. Paul,¹ Yeon Sun Kim,¹ Jennifer L. Gilbert,¹ Yasser S. Attiga,¹ Jackelyn A. Alva-Ornelas,¹ Derek W. Nickerson,¹ and Brigitte N. Gomperts^{1,3-5}

Both basal and submucosal gland (SMG) duct stem cells of the airway epithelium are capable of sphere formation in the in vitro sphere assay, although the efficiency at which this occurs is very low. We sought to improve this efficiency of sphere formation by identifying subpopulations of airway basal stem cells (ABSC) and SMG duct cells based on their aldehyde dehydrogenase (ALDH) activity. ALDH^{hi} ABSCs and SMG duct cells were highly enriched for the population of cells that could make spheres, while the co-culture of ALDH^{hi} differentiated cells with the ALDH^{hi} ABSCs increased their sphere-forming efficiency. Specific ALDH agonists and antagonists were used to show that airway specific ALDH isozymes are important for ABSC proliferation. Pathway analysis of gene expression profiling of ALDH^{hi} and ALDH^{lo} ABSCs revealed a significant upregulation of the arachidonic acid (AA) metabolism pathway in ALDH^{hi} ABSCs. We confirmed the importance of this pathway in the metabolism of proliferating ALDH^{hi} ABSCs using bioenergetics studies as well as agonists and antagonists of the AA pathway. These studies could lead to the development of novel strategies for altering ABSC proliferation in the airway epithelium.

Introduction

THE MOUSE PROXIMAL airway epithelium is maintained and repaired after injury by the action of at least two distinct epithelial progenitor cell populations, airway basal stem cells (ABSCs) of the surface epithelium and the duct cells of the submucosal glands (SMG) [1–5]. These progenitor cells are capable of self-renewal and of differentiating into the mature cell types of the airway to ensure efficient mucociliary clearance. Our understanding of these progenitor cell populations has increased greatly, thanks in large part to an in vitro sphere-forming assay that is used to assess the proliferation and differentiation potential of these progenitor cells [1–3,5]. These studies showed that ABSCs and SMG duct cells are capable of forming clonal spheres while non-ABSCs and non-duct cells do not. However, the very low incidence of sphere formation in this assay (range 0.6%–1%, average 0.75% ± 0.13% in our hands, 3% in others' hands [5], 10%–70% in other organs including the brain, prostate, and breast [6])

prompted us to try to find a marker to enrich for the subpopulations of ABSCs and duct cells with the ability to form spheres.

Aldehyde dehydrogenase (ALDH) activity has been shown in other tissues, such as hematopoietic tissue [7,8] and breast tissue [9], to delineate stem cell subpopulations with greater proliferative capacity and potentially a cancer stem cell phenotype [9–11]. In the lungs, *ALDH1A1* and *ALDH3A1* expression was found in normal airways and high expression of *ALDH1A1* and *ALDH3A1* was found in non-small cell lung cancer (NSCLC) [12]. Further, *ALDH1A1* expression was found to correlate with poorer prognosis in NSCLC and to mark a subpopulation of tumor cells [13].

There are more than 19 different isozymes of ALDH [14–16], and we hypothesized that functionally they play a crucial role in protecting the airways from aldehydes derived from endogenous and exogenous sources [17]. As the airways are constantly exposed to air pollution, which is a

¹Department of Pediatrics, Children's Discovery and Innovation Institute, David Geffen School of Medicine at UCLA, Mattel Children's Hospital, Los Angeles, California.

²Department of Biological Chemistry, Howard Hughes Medical Institute, David Geffen School of Medicine, University of California Los Angeles, Los Angeles, California.

³Division of Pulmonary and Critical Care Medicine, Department of Medicine, David Geffen School of Medicine at UCLA, Los Angeles, California.

⁴Broad Stem Cell Research Center at UCLA, Los Angeles, California.

⁵Jonsson Comprehensive Cancer Center at UCLA, Los Angeles, California.

*Current affiliation: Division of Pulmonary Medicine, Department of Medicine, Keio University Medical School, Tokyo, Japan.

major source of exogenous aldehydes, we reasoned that the cells of the airway epithelium would need to be enriched in ALDH to protect the body from toxic aldehyde effects [17]. We further speculated that cells with the greatest ability to withstand toxic aldehyde exposure would be the cells most likely to survive and proliferate for repair after injury.

Here, we identified high ALDH activity as a marker that enriches for proliferating ABSCs and SMG duct cells. We performed gene expression profiling of ALDH^{hi} and ALDH^{lo} ABSCs and non-ABSCs and found that one of the most significant differences was in the arachidonic acid (AA) metabolism pathway. We confirmed the importance of this pathway in selective proliferation of ALDH^{hi} ABSCs using bioenergetics studies and inhibition and activation of the pathway. Our work suggests that mechanistically, the ability of proliferating ABSCs to metabolize AA as an energy source is important when metabolic substrates are in short supply after airway injury.

Materials and Methods

Mice

Eight to ten week-old wild-type C57BL/6 and β -actin red fluorescent protein (RFP) (C57BL/6-Tg[ACTbERFP]1Nagy/J) mice were used for these experiments. Mice were housed and bred under the regulation of the Division of Laboratory Animal Medicine at the University of California, Los Angeles.

Fluorescence-activated cell sorting based on ALDH activity, sphere formation assay, and quantification of sphere number and size

Mouse tracheal epithelial cells were collected and sorted into ABSCs and non-ABSCs and SMG duct and non-duct cells as described previously [1,3]. Sorting was further performed based on the ALDH activity of airway epithelial cells using the Aldefluor[®] kit (Stem Cell Technologies) and was performed at the concentration of 1×10^6 cells/mL Aldefluor assay buffer, per the manufacturer's recommendations. Eight to ten tracheas were used per isolation and unless stated otherwise, 50,000 cells were seeded per transwell. Sphere formation efficiency was calculated as a percentage of sphere number to number of seeded cells. Sphere numbers and diameters were visually counted and measured from digital images from all transwells 2 weeks after seeding. At this time point, a colony of cells with a diameter of $>50 \mu\text{m}$ is considered a sphere. All experimental wells were run in triplicates and every experiment was repeated at least twice.

In vitro sphere cultures of wild type with RFP+ cell populations

Fluorescence-activated cell sorting (FACS)-sorted cells were resuspended in mouse tracheal epithelial cells (MTEC)/Plus media [18], and mixed 1:1 with growth factor-reduced Matrigel (BD Biosciences). Sorted RFP+ ALDH^{lo} ABSCs, ALDH^{lo} non-ABSCs, and ALDH^{hi} non-ABSCs were co-cultured with wild-type ALDH^{hi} ABSCs (50,000 cells/transwell). The number of spheres per well was counted on day 7 and 14 of culture. RFP+ spheres were detected with an inverted fluorescent microscope (Zeiss Axiovert).

Tracing the mitotically active ABSCs by labeling with the red fluorescent cell membrane linker PKH26

Primary sorted ABSCs were stained with PKH-26, a fluorescent dye with long aliphatic tails for incorporation in the cell membrane, using the PKH26 Red Fluorescent Cell Linker Kit (Sigma) according to the manufacturer's instructions. Two weeks later, spheres were digested and sorted based on PKH26 fluorescence and ITGA6 immunostaining.

Treating with ALDH agonists and antagonists

Sorted ABSCs or SMG duct cells were cultured on matrigel and treated with the broad-spectrum ALDH inhibitor, diethylaminobenzaldehyde (DEAB) (100–200 μM) or with specific ALDH1A1, ALDH2, and ALDH3 inhibitors, Acrolein (3 μM), Daidzin (100 μM), and AA (100 μM) or with agonists of ALDH2, and ALDH3; Alda-1 (100 μM), and Alda-89 (100 μM) (kind gift of Dr. Mochly-Rosen) at day 0 of in vitro culture or at day 7. Spheres were imaged and collected at days 14 and/or 21 of culture.

Quantitative real-time PCR

Total RNA was extracted from sorted cell populations using the RNeasy kit (Qiagen). cDNA was synthesized from all RNA samples using TaqMan reverse transcription reagents according to the manufacturer's protocol (Applied Biosystems). Quantitative real-time PCR (QPCR) was performed using a TaqMan Fast Universal PCR master mix according to the manufacturer's protocol (Applied Biosystems) and analyzed with the Step One real-time PCR system (Applied Biosystems) using predesigned primer/probe mixtures for *Gapdh*, *Aldh1a1*, *Aldh2*, and *Aldh3a1* (Applied Biosystems).

Western blots

Cell lysates obtained from sorted cells containing equivalents of total protein (10 μg) were resolved on a 12% sodium dodecyl sulfate-polyacrylamide gel, followed by transfer to nitrocellulose membranes (Bio-Rad). Membranes were blocked in skimmed milk in PBS buffer for 60 min followed by incubation with rabbit ALDH1A1, rabbit ALDH2 (Abcam), rabbit ALDH3A1 (Abgent), or rabbit anti- β -actin (Rockland Immunochemicals) (1:500 to 1:1,000 dilutions). Membranes were then washed and incubated with the appropriate horseradish peroxidase-coupled secondary antibodies (Bio-Rad) and the immunocomplexes were visualized using SuperSignal West Pico Chemiluminescent System (Thermo Scientific). The bands were quantified by densitometric scanning using ImageLab software Version 3.0 Build 11 (Bio-Rad).

RNA extraction and library manufacturing for RNA sequencing

RNA was extracted from sorted cells using the RNeasy Micro Kit (Qiagen). The cDNA was generated and amplified using the Ovation RNA-Seq V2 System (NuGEN). The resulting cDNA was sheared to 140–180 bp using the Covaris Focused-ultrasonicator with the following settings, duty cycle: 10%; intensity: 5; cycles per burst: 200; total time: 6 min.

The size range of the sheared cDNA was visualized and confirmed with bioanalyzer analysis prior to library construction. The sequencing libraries were prepared using the Encore Library System (NuGEN). The average sizes of the libraries were estimated with a bioanalyzer, and the concentrations of the libraries were measured on the Qubit™ fluorometer (Invitrogen).

RNA-sequencing read mapping and expression quantification

We first filtered the raw reads to remove low quality reads and reads containing sequencing adapters. Then, we aligned the filtered raw reads (single end, 50 bp in length) to the reference mouse genome (University of California, Santa Cruz release mm9) with the gapped aligner Tophat [19] (version 1.3.0) allowing up to two mismatches. The mouse gene model annotation (version of Mus_musculus .NCBIM37.63) was downloaded from the Ensembl database (ftp://ftp.ensembl.org/pub/current_gtf/mus_musculus/) and supplied to Tophat. Only uniquely aligned reads were considered for further analysis. Altogether, about 386 million reads were uniquely mapped and used in this study. The expression abundance of each individual gene and transcript was quantified by Cufflinks [20] (version 1.0.3) in the Fragments Per Kilobase of exon per Million (FPKM) unit fragments mapped together with confidence intervals. Cufflinks ran in the default parameters except that the annotated gene set was supplied using the `-G` option. We also measured the raw read count for each gene and transcript using customized scripts written in Perl.

Bioinformatic analysis

We performed the differential expression analysis using the R package, DESeq [21]. With this test, raw read counts were employed to model the negative binomial distribution of expression abundances of all genes and transcripts. We filtered out low expressing genes and transcripts by only keeping those that had at least one count per million in the samples. The multiple testing errors were corrected by the false discovery rate. In addition to the cutoff adjusted P -value < 0.05 , we also adopted an additional cutoff set as the expression ratio of above two-fold changes in expression values. In summary, we considered genes as differentially expressed genes if (1) the adjusted P -value was < 0.05 and (2) the expression ratio between two conditions was above two-fold.

Extracellular flux bioenergetic assay

Assays were performed in accordance with manufacturer's instructions (Seahorse Bioscience) and described previously [22]. Briefly, 40,000 sorted cells were seeded in extracellular flux 96-well cell culture microplates (Seahorse Bioscience) in 80 μ L of MTEC plus cell growth medium (with 0.01 μ M retinoic acid) and then incubated at 37°C/5% CO₂ for ~24 h. Assays were initiated by replacing the cell growth medium from each well with 200 μ L of Krebs-Henseleit buffer assay medium (Seahorse Bioscience) supplemented with 0.5 mM L-carnitine. The microplates were incubated at 37°C for 60 min to equilibrate the temperature and pH of the media before measurement. A Seahorse Bioscience instrument (model XF96) was used to measure the rate of change

of dissolved O₂ and pH in the media. Briefly, freshly prepared bovine serum albumin-complexed palmitate/AA was injected at a final concentration of 20 μ M in low glucose minimal medium supplemented with carnitine and the palmitate/AA oxidation rate was calculated as the increase in oxygen consumption above baseline. Oxygen consumption rate (OCR) was measured simultaneously for ~2 min in repeated cycles, to obtain a basal average. All OCR values were normalized to protein concentration using the Protein Assay reagent (Qubit fluorometer; Invitrogen) in all experiments. All wells were run in triplicates. The media formulations of the high glucose (25 mM), low glucose (5.56 mM), and no glucose medium were equal (Invitrogen 11995, 11885 and 11966). The very low glucose (2.78 mM) medium was prepared by mixing equal volumes of low and no glucose media.

Immunostaining of spheres

After 14–21 days of in vitro culture, matrigel discs containing the spheres were embedded in Histogel and then in paraffin for sectioning. Sections were processed and immunofluorescence was performed as previously described [1]. Primary antibodies used were Rabbit Keratin 5 (1:200; Covance), Goat polymeric immunoglobulin receptor (pIgR) (1:100; R&D Systems), Rabbit ALDH1/2 (1:100; Santa Cruz), Rabbit ALDH1A1 and Rabbit ALDH2 (1:100; Abcam), Rabbit ALDH3A1 (1:50; Abgent), Rabbit Keratin 14 (1:200; Epitomics), and Rat Ki67 (1:100; Dako). To detect mucus secretions in spheres, Alcian blue and Periodic Acid Schiff staining was performed, as previously described [1].

Lipoxygenase inhibition

Sorted ABSCs (60,000–80,000 cells per well) were cultured in Transwell membrane inserts (0.4 μ m pore size; Corning) on matrigel and MTEC/Plus media and treated with the specific lipoxygenase 12e and 15 inhibitor, ethyl 3,4-dihydroxybenzylidenecyanoacetate (DHBLCA; Sigma) using concentrations of 5, 10, 15, or 20 μ M for 14 days. Spheres were imaged, embedded, and sectioned. Immunofluorescence staining using a 1:200 dilution of anti-Ki67 (Dako), anti-Keratin 5 (Covance), and anti-pIgR (R&D Systems) was performed as previously described [1].

Statistical analysis

Data are presented as average \pm SEM. The two-tailed student's t -test was used for comparisons, with $P < 0.05$ considered statistically significant.

Results

ALDH activity enriches for proliferating ABSCs and SMG duct cells of the airway epithelium

Airway surface epithelial ABSCs and SMG duct cells of the mouse trachea demonstrate self-renewal and differentiation properties in vitro in the sphere formation assay [1,5]. We use the sphere formation assay as a surrogate to examine ABSC proliferation, and serial propagation of single cells from spheres allows an assessment of self-renewal [6]. The percentage of cells that give rise to spheres in our assay is $0.4\% \pm 0.2\%$ for Trop2+ sorted SMG duct cells and

0.6%±0.4% for Itga6+ /Trop2+ sorted ABSCs. We hypothesized that high ALDH activity would enrich for the progenitor cells within the ABSC and SMG duct cell populations. We therefore sorted ALDH^{hi} and ALDH^{lo} populations (Fig. 1i, ii) and cultured them in the sphere formation assay. The ALDH^{hi} ABSC population had a 10-

fold higher sphere-forming efficiency than the ALDH^{lo} ABSC population (Fig. 1iii, iv), while the ALDH^{lo} SMG duct cell population was essentially unable to form spheres (Fig. 1v, vi). However, culturing the ALDH^{hi} ABSCs or ALDH^{hi} SMG duct cells alone resulted in lower sphere-forming efficiency compared with culturing ALDH^{hi} and ALDH^{lo} populations

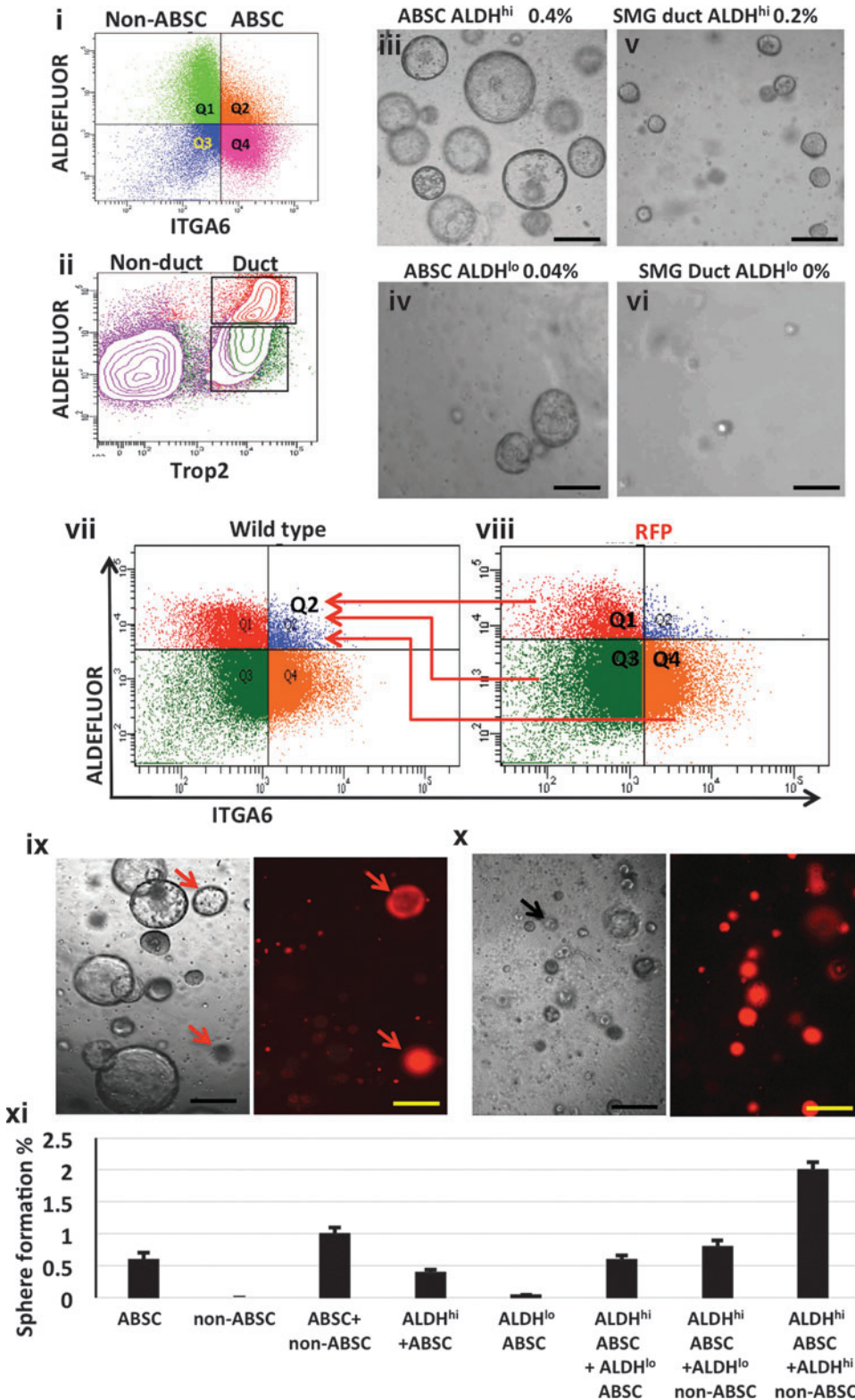


FIG. 1. ALDH^{hi} airway basal stem cells (ABSC) and duct cell populations are enriched for the sphere-forming airway epithelial cells. ABSC (i) and submucosal gland (SMG) duct (ii) cells were sorted based on their aldehyde dehydrogenase (ALDH) expression, using the Aldefluor assay. ALDH^{hi} ABSCs showed 10 times higher sphere formation efficiency (iii) compared with ALDH^{lo} ABSCs (iv). ALDH high (v) and low (vi) cells within the SMG duct cell population showed the same phenomenon. ALDH^{hi} ABSCs (Q2), ALDH^{lo} ABSCs (Q4), ALDH^{hi} non-ABSCs (Q1), and ALDH^{lo} non-ABSCs (Q3) were sorted from red fluorescent protein (RFP) mice. Then cells from RFP Q1, 3 and 4 were co-cultured with cells from wild-type Q2 (vii, viii). (ix) Shows that the coculture of wild-type ALDH^{hi} ABSCs with RFP ALDH^{hi} non-ABSCs caused marked increase in sphere-formation efficiency with almost all spheres originating from the wild-type ALDH^{hi} ABSCs. Very few spheres originated from the ALDH^{hi} non-ABSCs (red arrows). (x) Shows similar results to ix with the coculture of RFP ALDH^{hi} ABSCs with wild-type ALDH^{hi} non-ABSCs. In this experiment, one sphere originated from the wild-type ALDH^{hi} non-ABSC population (black arrow). (xi) Bar graph showing the sphere formation efficiency from the different populations. Scale bar = 100 μm.

together (0.2% for duct cells down from 0.4%, and 0.4% for ABCs down from 0.6%, $P < 0.001$).

ALDH^{hi} non-ABSCs of the airway epithelium promote ALDH^{hi} ABSC proliferation and sphere formation

We hypothesized that the ALDH^{lo} ABSC population of the airway epithelium might contain an essential cell population required for supporting the sphere-forming progenitor cells within the ALDH^{hi} ABSC population. To examine this, we sorted airway epithelial cells into four populations based on low and high expression of Itga6 and ALDH activity, and then cultured the sorted populations independently or together to determine their sphere forming potential. Sorted total ABCs had a sphere-forming efficiency of 0.6%. While the ALDH^{hi} ABCs were the only population of cells capable of independent sphere formation, the efficiency decreased to 0.4%. When we co-cultured the four populations, the efficiency increased to 1% ($P < 0.05$). This implies that there is a subpopulation of cells other than the ALDH^{hi} ABCs that promotes its proliferation to form spheres. To identify this subpopulation, we sorted ALDH^{lo} ABCs, ALDH^{lo} non-ABCs, and ALDH^{hi} non-ABCs from mice that ubiquitously express RFP and co-cultured each subpopulation separately with ALDH^{hi} ABCs sorted from wild-type mice (Fig. 1vii, viii). We then assessed the sphere-forming efficiency of the different cell populations by their expression of RFP (Fig. 1ix–xi). We found that the presence of ALDH^{lo} ABCs or ALDH^{lo} non-ABCs in culture with the ALDH^{hi} ABCs resulted in a modest increase in sphere-forming efficiency compared with culturing ALDH^{hi} ABCs alone under equal seeding densities (increased from $0.4\% \pm 0.04\%$ to $0.6\% \pm 0.06\%$ ($P < 0.005$)) (Fig. 1xi). However, the presence of ALDH^{hi} non-ABCs in culture with the ALDH^{hi} ABCs resulted in a marked increase in sphere-forming efficiency compared with culturing ALDH^{hi} ABCs alone [increased from $0.4\% \pm 0.04\%$ to $2\% \pm 0.12\%$ ($P < 0.0005$), Fig. 1ix–xi]. In all co-culture experiments, ALDH^{hi} ABCs remained the sphere-forming population of cells, as the majority of spheres that formed were RFP negative (Fig. 1ix–xi). These data indicate that the ALDH^{hi} ABC population is highly enriched for a progenitor population and that their regenerative capacity is increased by the addition of non-sphere forming cells, which are highly enriched within the ALDH^{hi} non-ABC population.

High ALDH expression does not select for the proliferating ABSC populations with serial propagation of spheres

We wanted to examine whether high ALDH expression would continue to mark for the ABCs after serial propagation of spheres in vitro. First, we wanted to demonstrate that ABCs are the cells that are responsible for the self-renewal and propagation of spheres with serial passaging. We therefore fluorescently labeled sorted ABCs with the PKH-26 membrane linker dye to track the serial dilution of the dye with serial mitotic events [23]. After visually confirming homogenous PKH staining of all cells, we cultured the labeled ABCs for 2 weeks before dispersing the spheres into single cell suspensions and sorting them into Itga6^{hi}/PKH^{lo}, Itga6^{hi}/PKH^{hi} (ABCs with and without frequent

mitoses) and Itga6^{lo}/PKH^{lo}, Itga6^{lo}/PKH^{hi} (non-ABCs with and without frequent mitoses). When these four populations were re-cultured, Itga6^{hi}/PKH^{lo} cells (ABCs with frequent mitoses) had significantly higher sphere-forming efficiency than other cell populations ($P < 0.05$) indicating that the ABCs that were mitotically active continued to be the sphere-forming cells with serial passaging in our in vitro assay and that more quiescent cells did not make spheres (Supplementary Fig. S1i, ii; Supplementary Data are available online at www.liebertpub.com/scd). Then, to determine whether ALDH activity continued to mark mitotically active sphere-forming cells with serial passaging, we sorted passaged Itga6^{hi} ABCs into ALDH^{hi} and ALDH^{lo} populations and re-cultured them in the sphere assay. While ALDH activity marked the sphere-forming cells of the airway epithelium, there were no differences in the sphere-forming potential between ALDH^{hi} and ALDH^{lo} cells in the passaged cell cultures (Supplementary Fig. S1iii, iv).

Identification and validation of ALDH isoforms that are highly expressed in proximal airway epithelium

To identify which ALDH isozymes are important in the airway epithelium, we examined gene expression profiles of ALDH^{hi} non-ABCs, ALDH^{hi} ABCs, and ALDH^{lo} ABCs using high-throughput RNA sequencing (RNA-seq) (Table 1). Differentially expressed candidate genes from the RNA-seq data were validated by QPCR, (Supplementary Fig. S2). The RNA-seq data showed that *Aldh1a1*, *Aldh2*, *Aldh3a1*, and *Aldh1a7* were the most highly expressed ALDH isozymes in mouse airways and lung, which is similar to what we found in our previous RNA microarray studies [1] and in a previously published study [24]. Because *Aldh1a7* has no corresponding human gene, we restricted our further studies to *Aldh1a1*, *Aldh2*, and *Aldh3a1*. We performed immunostaining for these three ALDHs in mouse tracheal sections and found that all proximal airway epithelial cells expressed these three ALDH isoforms although ALDH2 and ALDH3A1 had higher expression in ABCs and SMG duct cells while ALDH1A1 had higher expression in non-ABCs (Fig. 2i–iii). We also compared protein and RNA expression of *Aldh1a1*, *Aldh2*, and *Aldh3a1* in ALDH^{hi} ABC, ALDH^{lo} ABC, and ALDH^{hi} non-ABC populations. We confirmed that the protein and gene expression of these three ALDH isoforms were higher in the ALDH^{hi} cells than the ALDH^{lo} cells (Fig. 2iv, v).

Effect of inhibition and induction of the ALDH isoforms on ABSC sphere formation, proliferation, and differentiation capabilities

To examine the role of ALDH activity in sphere formation, we treated sorted ABCs or SMG duct cells with the broad-spectrum ALDH inhibitor, DEAB (100–200 μ M), at day 0 of in vitro culture (before sphere formation occurs) or at day 7 of culture, after spheres had already formed but were still small in size and undergoing rapid proliferation [1]. We found that treatment at day 0 markedly diminished sphere formation (Fig. 3ii), while treatment at day 7 (Fig. 3iii), after spheres had already formed, resulted in a decrease in sphere size compared with control (Fig. 3i–iii, Supplementary Table S1 and Supplementary Fig. S3).

TABLE 1. RELATIVE GENE EXPRESSION (RPKM) OF ALDH ISOZYMES FROM RNA-SEQ OF SUBPOPULATIONS OF MOUSE AIRWAY EPITHELIAL CELLS

Gene	Non-basal ALDH ^{hi}	Non-basal ALDH ^{hi}	Basal ALDH ^{hi}	Basal ALDH ^{hi}	Basal ALDH ^{lo}	Basal ALDH ^{lo}
<i>Aldh1a1</i>	1863.88	1621.72	851.606	765.868	327.942	275.356
<i>Aldh3a1</i>	115.371	133.11	35.8555	67.7412	54.0426	51.4267
<i>Aldh1a7</i>	74.8274	54.5831	39.3715	33.0375	27.9833	18.2261
<i>Aldh2</i>	52.4179	69.4437	39.9574	31.7235	30.4623	35.5069
<i>Aldh3a2</i>	39.0079	33.9991	115.14	29.953	16.3966	22.787
<i>Aldh6a1</i>	14.2279	9.24365	14.8621	18.8626	17.3809	17.7573
<i>Aldh16a1</i>	14.1157	16.6422	14.8939	9.55912	7.451	4.86497
<i>Aldh18a1</i>	9.84418	11.2891	7.62724	2.78219	4.88272	2.31466
<i>Aldh3b1</i>	9.8247	3.14901	3.34813	2.88716	1.26869	1.76851
<i>Aldh7a1</i>	8.43542	11.1004	8.5909	15.6174	11.0085	35.9611
<i>Aldh9a1</i>	5.7111	8.55623	6.00172	5.67304	7.47862	4.16696
<i>Aldh4a1</i>	4.41157	7.01552	3.01155	5.91411	3.17983	6.53516
<i>Aldh5a1</i>	4.34505	4.95532	3.63737	2.37622	1.84831	1.72413
<i>Aldh11</i>	3.71107	3.0356	1.3466	1.69656	1.02243	0.957952
<i>Aldh3b2</i>	0.876781	10.3994	5.80983	1.31737	0.995072	1.16484
<i>Aldh1a3</i>	0.574336	0.190996	0.451274	0.322906	0.0961869	0.0623636
<i>Aldh1a2</i>	0.461689	0.129546	0.36822	0.250303	0	0
<i>Aldh112</i>	0.395049	2.0586	0.0325728	0.218406	0.233396	0.468432
<i>Aldh1b1</i>	0.324425	0.0910306	0.181121	0.0947076	0.0550123	0.076091
<i>Aldh8a1</i>	0.132232	0.0185515	0	0	0.0771887	0

Two samples of each population are represented from two different sorts. ALDH, aldehyde dehydrogenase; RNA-seq, RNA sequencing.

To further assess the effect of individual ALDH isozymes on ABSC sphere formation and proliferation, we similarly treated sorted cells in culture with specific ALDH2, ALDH1A1, and ALDH3 inhibitors namely, daidzin [25], acrolein [26] and high dose AA [27], respectively. These three agents had similar effects to DEAB, that is, treatment at day 0 markedly diminished sphere formation (data not shown), while treatment at day 7 after spheres had already formed resulted in a decrease in sphere size (Fig. 3iv–vi, Supplementary Table S1 and Supplementary Fig. S3).

To directly examine the effect of ALDH inhibition on cell proliferation, we immunostained sections of spheres that were previously treated with ALDH inhibitors for proliferating cell nuclear antigen and Ki-67 expression and counted the number of proliferating cells. We found that ALDH inhibition significantly reduced the number of proliferating cells within spheres (Supplementary Table S1 and Supplementary Fig. S3ii). We used trypan blue exclusion to confirm that all ALDH antagonists used at the specified concentrations had no effect on cell death compared to the vehicle treated control (data not shown).

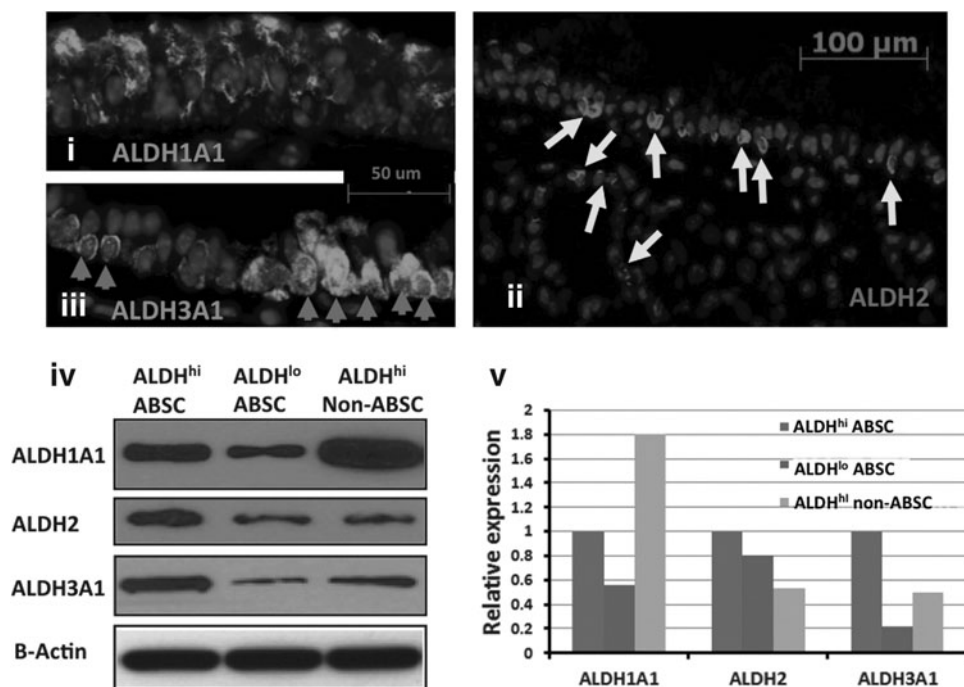


FIG. 2. Expression of ALDH1A1, ALDH2, and ALDH3A1 in the airway epithelium. Immunofluorescent staining of mouse trachea for ALDH1A1 (i), ALDH2 (ii), and ALDH3A1 (iii). Arrows point to positively stained basal and submucosal gland duct cells. (iv) Western blot for ALDH1A1, ALDH2, and ALDH3A1 on protein collected from the fluorescence-activated cell sorted ALDH^{hi} and ALDH^{lo} ABSC and ALDH^{hi} non-ABSC (differentiated) cell populations. (v) Densitometry quantification of the bands in (iv). The expression levels of ALDH1A1, ALDH2, and ALDH3A1 in the ALDH^{lo} ABSCs and ALDH^{hi} non-ABSCs are shown relative to their expression in ALDH^{hi} ABSCs. Protein levels were normalized with B-Actin.

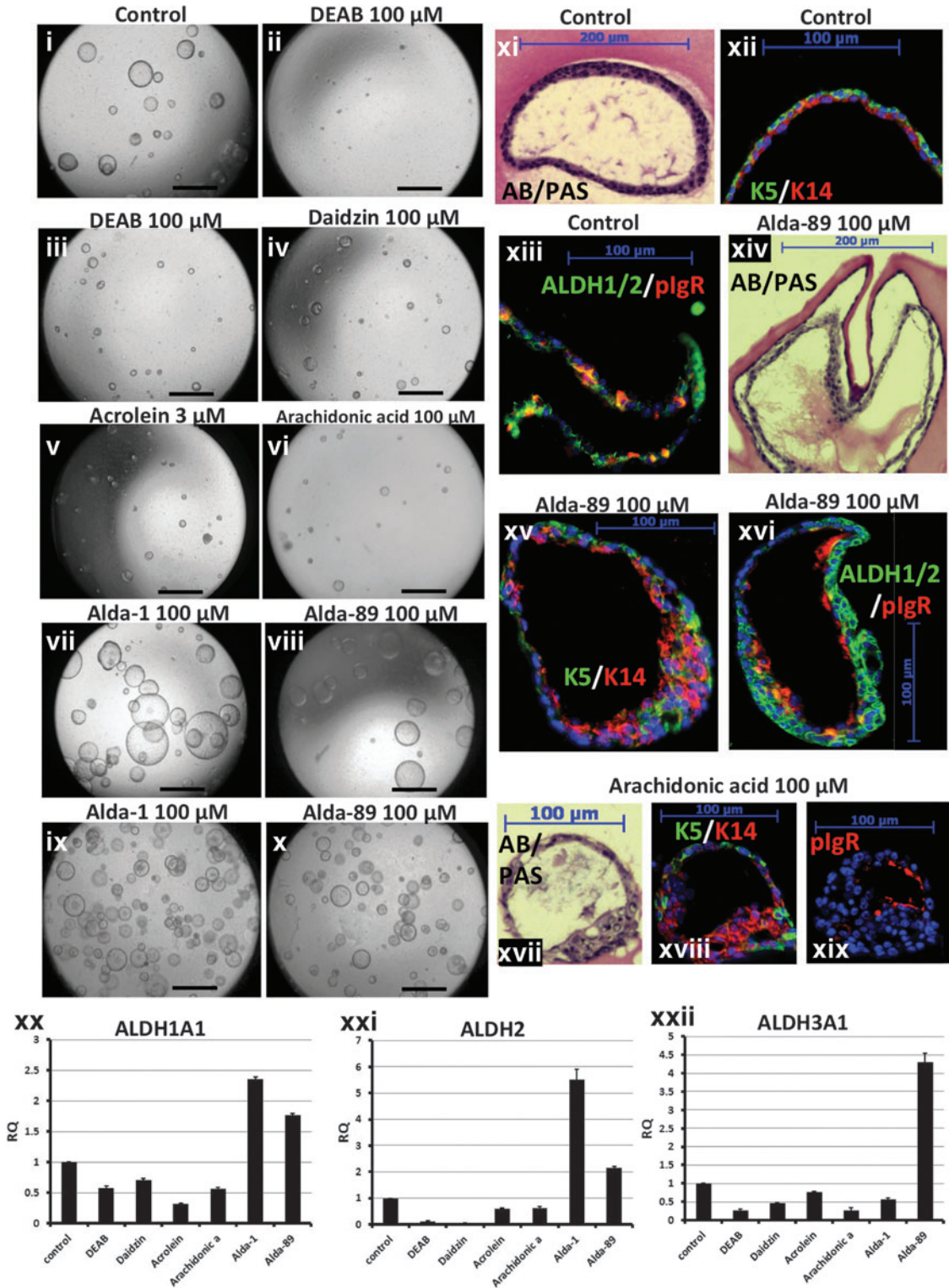


FIG. 3. Effect of inhibition and induction of the ALDH isoforms on stem/progenitor cell proliferation and differentiation capabilities. (i–x) Images taken 14 days after seeding of ABSCs at equal densities. (i) Vehicle-treated. (ii) 100 μ M diethylaminobenzaldehyde (DEAB) at culture day 0. (iii–viii) 100 μ M DEAB, daidzin, acrolein, arachidonic acid (AA), Alda-1, and Alda-89 at culture day 7. (ix, x) 100 μ M Alda-1 and Alda-89 at culture day 0, Scale bar = 500 μ m. (xi, xiv, xvii) Alcian blue/Periodic Acid Schiff staining, (xii, xv, xviii) immunofluorescent staining for Keratin 5 and 14 and (xiii, xvi, xix) immunofluorescent staining for polymeric immunoglobulin receptor (pIgR) and ALDH1/2 from vehicle-treated control, Alda-89-treated well and AA treated well, respectively. (xx–xxii) Quantitative real-time PCR (QPCR) assessment of the effect of each agonist and antagonist on relative gene expression of *Aldh1a1*, *Aldh2*, and *Aldh3a1*.

To examine the effects of agonists of these ALDH isoenzymes on sphere formation and proliferation, we used Alda-1 and Alda-89, two recently developed small molecule agonists for ALDH2 and ALDH3, respectively [28,29]. Treating sorted ABSCs at day 7 with Alda-1 or Alda-89 produced significantly larger spheres compared to controls with the average sphere diameter increasing from the untreated average size of $110 \pm 34 \mu\text{m}$ to $132 \pm 42 \mu\text{m}$ and $128.5 \pm 54 \mu\text{m}$ (increases of 19.7% and 16.5% respectively) ($P < 0.004$ and $P < 0.005$ respectively) (Fig. 3vii, viii and Supplementary Fig. S3), while treatment with these agonists at day 0 produced larger numbers of spheres and larger diameter spheres compared to untreated controls (Fig. 3ix, x).

We next examined whether altering ALDH levels in growing spheres affected the differentiation ability of ABSCs. Compared to untreated controls, all ALDH agonists and antagonists, in spite of affecting ABSC proliferation in the sphere assay, did not affect differentiation toward the secretory lineage as both mucus and serous secretions were detectable 2 weeks after treatment (Fig. 3xiv–xvi represent agonists and xvii–xix represent antagonists).

To confirm the direct inhibitory or inductive effect of these antagonists and agonists on ABSCs in our assays, *Aldh1a1*, *Aldh2*, and *Aldh3a1* expression in the treated or control spheres were examined using QPCR. Alda-1 and Alda-89 significantly induced *Aldh2* and *Aldh3a1* expression, respectively. However, Alda-1 and Alda-89 treatment also moderately induced *Aldh1a1* expression. The antagonists acrolein, daidzin, and high concentrations of AA, were the most efficient in reducing the expression of *Aldh1a1*, *Aldh2*, and *Aldh3a1*, respectively. However, the expression of each gene was also variably reduced by all the other inhibitors (Fig. 3xx–xxii), indicating a lack of specificity for induction of each

isozyme, at the concentrations used. Taken together, these results demonstrate that ALDH activity is not only a marker of the proliferative subpopulation of ABSCs, but also functionally important in sphere formation and cell proliferation in the sphere assay.

ALDH^{hi} ABSCs have a few key gene expression profile differences when compared to the ALDH^{lo} ABSCs

Analysis of the RNA-seq data comparing differentially expressed genes between ALDH^{hi} and ALDH^{lo} ABSCs revealed that ~200 genes were significantly differentially expressed between the two cell populations, despite the fact that functionally only the sorted ALDH^{hi} cells could produce spheres in culture (Fig. 4i. *Gene Expression Omnibus* accession number pending). Kegg pathway analysis of the RNA-seq data revealed that two of the pathways that were most significantly upregulated in the sphere-forming ALDH^{hi} ABSCs versus non-sphere-forming ALDH^{lo} non-ABSCs were the PPAR signaling pathway (*Cd36*, *Ppara*), and the AA metabolism pathway (lipoxygenases 15 and 12e) (Fig. 4ii).

Differential metabolism of AA by subpopulations of ABSCs

Based on the RNA-seq data, we sought to determine whether ALDH^{hi} ABSCs are more efficient than ALDH^{lo} ABSCs in utilizing AA as a metabolic substrate. We therefore sorted ALDH^{hi} ABSC, ALDH^{lo} ABSC, ALDH^{hi} non-ABSC, and ALDH^{lo} non-ABSC subpopulations and measured the change in their OCR after incubating cells with an empirically set standard concentration of the fatty acid, Palmitate (20 μM) or

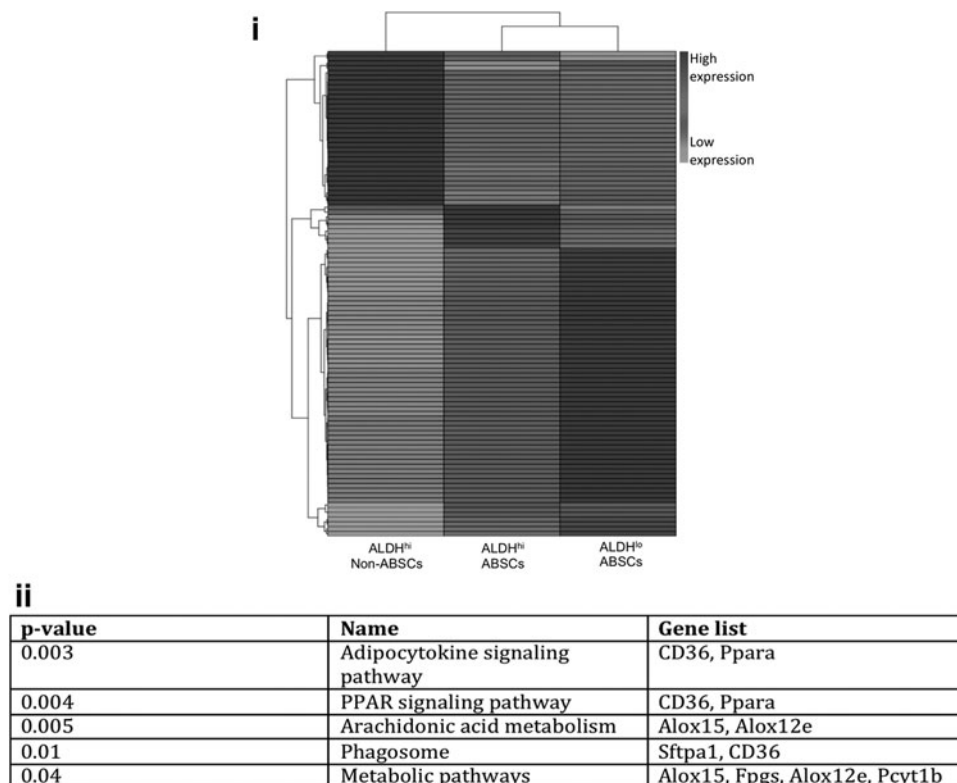


FIG. 4. Analysis of RNA-sequencing (RNA-seq) data from sorted ALDH^{hi} ABSCs, ALDH^{lo} ABSCs, and ALDH^{hi} non-ABSCs. **(i)** Heatmap demonstrating the top 100 differentially expressed genes between ALDH^{hi} and ALDH^{lo} subpopulations. **(ii)** Table demonstrating Kegg pathway analysis of RNA-seq data for the pathways that are most significantly upregulated in the ALDH^{hi} ABSC sphere-forming cells versus ALDH^{lo} non-sphere-forming cells.

the same concentration of AA using the XF96 Seahorse bioenergetic flux analyzer. In the presence of AA, the OCR values of ALDH^{hi} ABSCs increased two-fold ($200\% \pm 6.4\%$ $P < 0.01$) relative to the basal respiration OCR (Fig. 5i). However, ALDH^{lo} ABSCs showed only a mild increase ($31\% \pm 3.9\%$ $P < 0.2$) in OCR as a result of AA metabolism. In contrast, the differentiated non-ABSC subpopulation, which is highly metabolic due to production of mucus and serous secretions and cilia motility, did not utilize AA as a substrate for oxidative phosphorylation (Fig. 5i). These data suggest that the subpopulation of ABSCs with ALDH^{hi} activity might be better equipped to utilize AA as a substrate compared to the ALDH^{lo} ABSCs and non-ABSCs.

The ability of ABSCs to utilize AA as a source of energy in the presence or absence of glucose

We hypothesized that during airway injury when glucose levels are low due to an interruption of blood supply or inflammation, progenitor cells would require an alternative energy source to proliferate rapidly and repair the airway. We therefore tested whether ABSCs would have the ability to utilize AA as an energy source when glucose is limited. The Dulbecco's modified Eagle's medium/F12 cell culture medium that we routinely use to grow airway cells in vitro has a supraphysiologic glucose concentration of 25 mM. Culturing the cells with a normoglycemic glucose concentration (5.56 mM) in the medium will expose cells to increasing hypoglycemia until the next medium change. To examine the effects of varying concentrations of glucose on ABSC sphere formation, we cultured sorted ABSCs with the usual high glucose medium until spheres were visible in all wells, then continued culture using the same high glucose (25 mM) medium, low glucose (5.56 mM), or very low glucose (2.78 mM) medium for seven more days. We found that spheres exposed to low and very low glucose had a statistically significant decrease in sphere size compared with spheres grown in high glucose medium (Fig. 5ii, $P < 0.05$). The lower glucose medium had no effect on sphere-forming efficiency or on differentiation of cell types in the spheres. Prior to testing the ability of ABSCs to utilize AA as a metabolic substrate when glucose levels are low, we examined a dose course of AA to identify the optimum concentration at which AA causes a positive OCR using the XF96 Seahorse bioenergetic flux analyzer. We found that 60 μ M or less of AA produced induction in OCR while 100 μ M or more induced a down turn of OCR (data not shown). Therefore, we repeated the high, low, and very low glucose treatment experiment described above with AA supplementation. We found that 60 μ M AA supplementation increased the average sphere diameter in the high, low, and very low glucose treatments (Fig. 5ii) ($P < 0.0001$, $P < 0.001$, and $P < 0.05$ respectively). Thus, AA is an additional substrate for ALDH^{hi} ABSCs that may be especially important when glucose is limited.

Inhibition of lipoxygenases-12e and -15 prevents ABSC sphere formation and proliferation

We found that ALDH^{hi} ABSCs have increased lipoxygenase 12e and 15 gene expression and utilize AA as a metabolic substrate more efficiently than the ALDH^{lo} ABSC population. Therefore, to further examine the role of AA metabolism in ABSC sphere formation and proliferation, we inhibited lipoxygenases-12e (Alox12e or 8-LOX) and -15

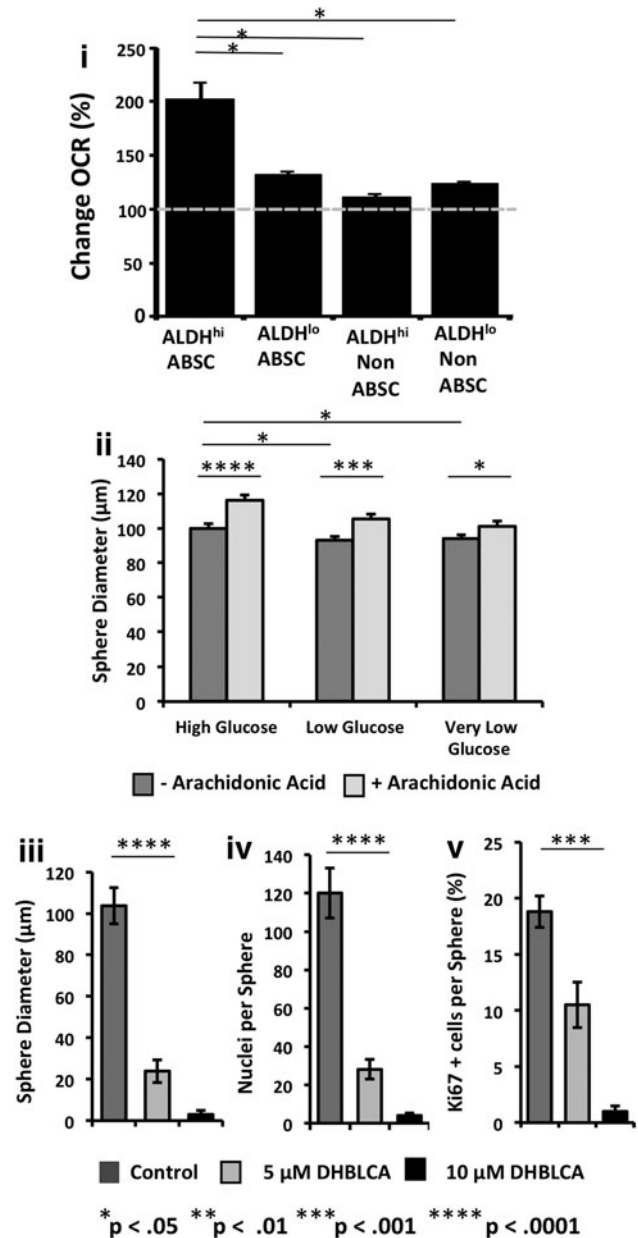


FIG. 5. AA metabolism in airway epithelial cell subpopulations. (i) Airway epithelial cells were sorted into ALDH^{hi} ABSC, ALDH^{lo} ABSC, ALDH^{hi} non-ABSC, and ALDH^{lo} non-ABSC subpopulations and cultured with AA as the only substrate. The change in oxygen consumption rate (OCR) was measured as a result of AA metabolism by each subpopulation. Dotted line shows % basal respiration before injection of AA. Data are expressed as mean \pm S.D. ($n=3$), (ii) Spheres grown under conditions of normal, low, or very low glucose concentrations showed an increase in stem/progenitor cell proliferation with larger sphere diameter with the addition of AA ($P < 0.0001$ for high glucose, $P < 0.001$ for low glucose, $P < 0.05$ for very low glucose). Spheres exposed to low and very low glucose showed a decrease in sphere size compared to spheres grown in high glucose medium ($P < 0.05$). (iii-v) Specific inhibition of lipoxygenases-12e and -15 with ethyl 3,4-dihydroxybenzylidenecyanoacetate (DHBLCA) resulted in a dose-dependent decrease in ABSC proliferation with a decrease in sphere diameter, nuclei per sphere, and reduced Ki67 expression ($P < 0.0001$ and $P < 0.001$ respectively).

(Alox15), the two lipoxygenases that were significantly upregulated in our RNA-seq data. We used the specific lipoxygenase 12e and 15 inhibitor, DHBLCA in the sphere-forming assay. We performed a dose course and found that at a concentration of 20 μ M DHBLCA, there was complete inhibition of sphere formation, although the cells were viable (data not shown). At lower DHBLCA concentrations, sphere formation did occur but the spheres were smaller in size and fewer in number (Fig. 5iii, iv, $P < 0.0001$, and data not shown). To evaluate the effect of DHBLCA on cell proliferation, treated spheres were embedded, sectioned, and immunostained for Ki67. We found decreased cell proliferation when spheres were treated with 5 and 10 μ M DHBLCA (Fig. 5v, $P < 0.001$ and Supplementary Fig. S4).

Discussion

Here, we show that high ALDH activity is a marker that enriches for the population of ABSCs that proliferate to generate spheres in vitro. In addition to being a marker, the ALDH activity within the ABSCs is functionally important for their ability to proliferate to form spheres. One mechanism for this appears to be the ability of ALDH^{hi} ABSCs to utilize AA more efficiently than other cell populations in the airway epithelium.

Aldehydes are derived from endogenous (eg, lipid peroxidation) and exogenous sources (eg, smoke) that form DNA adducts in cells and are therefore toxic to DNA [17]. ALDHs provide an efficient system for removal of aldehydes, which is critical to protect cells. As smoke is a well-known source of aldehydes, the airway epithelial cells are required to efficiently remove aldehydes to avoid their toxicity. We therefore speculate that ALDHs play an important role in protecting the airway epithelium, in addition to being markers of proximal ABSC populations. This is supported by the results of our in vitro experiments in which global ALDH inhibition interfered with ABSC proliferation. Further, ABSC proliferation increased when cultured with ALDH agonists, suggesting a functional role for ALDHs in ABSC repair after injury.

There are 19 different ALDH isozymes [14–16], which likely speak for their importance in the body, but here we identified and characterized the expression pattern of the three most highly expressed ALDH isozymes in the airway epithelium. In mouse tracheal sections, we found expression of ALDH2 and ALDH3A1 in ABSCs and SMG duct cells and expression of ALDH1A1 in non-ABSCs. Of note, none of the chemical or small molecule agonists [30,31] and antagonists [25,26,32] that we used to specifically perturb ALDH1A1, ALDH2, or ALDH3A1 isozyme levels were completely specific for these isoforms, suggesting overlapping roles. In addition, it is possible that the agonists and antagonists that we used to target specific ALDH isoforms may have exerted their effect on specific ALDH isozymes early on in the time course of the in vitro cultures and other ALDH isozymes may have been upregulated or downregulated to compensate for the lack of ALDH activity. It is also possible that these ALDH isozyme specific agonists and antagonists have dose-dependent effects on specificity that we did not test for in our system.

We used the “Aldefluor fluorescent reagent system” to detect ALDH activity in airway epithelial cells. Although

ALDH1A1 is considered to be the main isozyme detected by Aldefluor and inhibited by DEAB, it has been recently shown that Aldefluor and DEAB are not specific for isoform ALDH1A1, as they can also detect and inhibit other isoforms like ALDH1A2 and ALDH2 [32]. In addition, the full range of ALDH isozymes that oxidize Aldefluor are as yet unknown. Our data also show that within ABSCs, ALDH2 and ALDH3A1, in addition to ALDH1A1, oxidize Aldefluor.

Despite the fact that multiple ALDH isozymes appear to have similar functions, it is important to note that mutations in the human *ALDH2* gene are well described and in addition to suffering from flushing with alcohol, these patients are known to be at higher risk for squamous cancers, especially oropharyngolaryngeal, esophageal, gastric and lung cancer [33–37]. We speculate that because the airway epithelium is exposed to a large amount of exogenous aldehydes from smoke, loss of ALDH2 function may lead to aberrant repair and this together with the reduced ability to clear toxic aldehydes may predispose to lung cancer.

While high Aldefluor activity was important for determining which population of freshly sorted cells was capable of sphere formation, this was not the case with serial propagation of the spheres. The inability of high Aldefluor activity to select for ABSCs with self-renewal capacity during serial propagation in the sphere assay is consistent with observations in skeletal muscle progenitors, mesenchymal stem cells, and endothelial cells showing that *Aldh* expression is occasionally uncoupled from functional activity when cells are propagated in culture [38]. This may reflect the change in cellular microenvironment in the in vitro culture system and/or the reduction in aldehyde exposure in culture.

The concept of a “niche” cell in the epithelium that provides environmental cues and possibly paracrine factors has been established in the colon, where Paneth cells have been found to promote gut stem cell sphere formation [39]. Here, we found that a cell in the ALDH^{hi} non-ABSC population promotes sphere formation. This is further supported by our previous studies where we found that the sphere-forming efficiency of ABSCs was 2.1% \pm 0.6% [1]. However, since we have become stricter with our gating system for FACS, the sphere-forming efficiency in our current experiments has decreased. It is possible that in our earlier gating strategy, some non-ABSCs were included in the sort (including the niche cells that we are describing here) and enhanced the sphere formation that we previously described [1].

AA is a polyunsaturated fatty acid that is present in cell plasma membranes and is a lipid second messenger involved in cell signaling and inflammation. AA is derived from membranes by the action of Phospholipase A2 (PLA₂) and is a precursor of the eicosanoids. It has been proposed that cellular injury to the airway results in prolonged activation of PLA₂, resulting in hydrolysis of plasma membrane phospholipids and release of AA [40]. In our RNA-seq comparison of ALDH^{hi} and ALDH^{lo} ABSCs, we found upregulation of lipoxygenases-12e and -15, implying that AA may be an important energy source for ALDH^{hi} ABSCs. We showed that the addition of AA to ABSCs enhanced proliferation and this could be blocked with lipoxygenase inhibition. This suggests that following severe airway injury, when the blood supply may be interrupted and glucose supply is low, ALDH^{hi} ABSCs may utilize AA in the local environment to facilitate proliferation for repair. Interestingly, the overexpression of

lipoxigenase-15 in transgenic mice resulted in hyperplasia of prostate basal cells [41]. Further, lipoxigenases-12e and 15 have been linked to epithelial proliferation in corneal repair after injury [42]. In addition, asthmatics have been found to have high lipoxigenase levels in their airways and leukotriene inhibitors are clinically used in these patients to reduce inflammation, as well as reduce bronchial and vascular constriction. In light of our studies, we speculate that some of the epithelial cell proliferation and remodeling seen in asthma may arise from abnormally high lipoxigenase expression in ABSCs. This is supported by the fact that mice lacking lipoxigenase-12/15 have reduced airway epithelial proliferation in addition to reduced inflammation [43].

Conclusion

We have shown that ALDHs play a functional role in ABSC proliferation and perturbation of these enzyme levels alters proliferation in the sphere assay. In addition, we found that the specific isozymes of ALDH, ALDH1A1, ALDH2, and ALDH3A1 are highly enriched in the airway epithelium. Mechanistically, when comparing transcriptional profiles between ALDH^{hi} and ALDH^{lo} ABSC populations, we found that the AA metabolism pathway, specifically via lipoxigenases-12e and -15, is upregulated in the ALDH^{hi} ABSCs and that this promotes proliferation of these cells. We speculate that AA metabolic pathway plays a critical role in repair of the airway epithelium after injury.

Acknowledgments

We would like to acknowledge the UCLA Broad Stem Cell Research Center High-Throughput Sequencing Core Resource and the UCLA Broad Stem Cell Research Center FACS Core Resource. We would like to thank Dr. Mochly-Rosen for the Alda-1 and Alda-89 reagents. Acknowledgment of grants, equipment, or drugs for research support: CIRM RN2-00904-1, R01 HL094561, American Thoracic Society/COPD Foundation ATS-06-065, the Concern Foundation, the UCLA Jonsson Comprehensive Cancer Center Thoracic Oncology Program/Lung Cancer SPORE, the University of California Cancer Research Coordinating Committee, and the Gwynne Hazen Cherry Memorial Laboratories (BG).

Author Disclosure Statement

No competing financial interests exist.

References

- Hegab AE, VL Ha, JL Gilbert, KX Zhang, SP Malkoski, AT Chon, DO Darmawan, B Bisht, AT Ooi, et al. (2011). Novel stem/progenitor cell population from murine tracheal submucosal gland ducts with multipotent regenerative potential. *Stem Cells* 29:1283–1293.
- Hegab AE, VL Ha, DO Darmawan, JL Gilbert, AT Ooi, YS Attiga, B Bisht, DW Nickerson and BN Gomperts. (2012). Isolation and *in vitro* characterization of Basal and submucosal gland duct stem/progenitor cells from human proximal airways. *Stem Cells Transl Med* 1:719–724.
- Hegab AE, VL Ha, YS Attiga, DW Nickerson and BN Gomperts. (2012). Isolation of basal cells and submucosal gland duct cells from mouse trachea. *J Vis Exp* e3731.
- Hong KU, SD Reynolds, S Watkins, E Fuchs and BR Stripp. (2004). Basal cells are a multipotent progenitor capable of renewing the bronchial epithelium. *Am J Pathol* 164:577–588.
- Rock JR, MW Onaitis, EL Rawlins, Y Lu, CP Clark, Y Xue, SH Randell and BL Hogan. (2009). Basal cells as stem cells of the mouse trachea and human airway epithelium. *Proc Natl Acad Sci U S A* 106:12771–12775.
- Pastrana E, V Silva-Vargas and F Doetsch. (2011). Eyes wide open: a critical review of sphere-formation as an assay for stem cells. *Cell Stem Cell* 8:486–498.
- Armstrong L, M Stojkovic, I Dimmick, S Ahmad, P Stojkovic, N Hole and M Lako. (2004). Phenotypic characterization of murine primitive hematopoietic progenitor cells isolated on basis of aldehyde dehydrogenase activity. *Stem Cells* 22:1142–1151.
- Hess DA, L Wirthlin, TP Craft, PE Herrbrich, SA Hohm, R Lahey, WC Eades, MH Creer and JA Nolte. (2006). Selection based on CD133 and high aldehyde dehydrogenase activity isolates long-term reconstituting human hematopoietic stem cells. *Blood* 107:2162–2169.
- Ginestier C, MH Hur, E Charafe-Jauffret, F Monville, J Dutcher, M Brown, J Jacquemier, P Viens, CG Kleer, et al. (2007). ALDH1 is a marker of normal and malignant human mammary stem cells and a predictor of poor clinical outcome. *Cell Stem Cell* 1:555–567.
- Pearce DJ, D Taussig, C Simpson, K Allen, AZ Rohatiner, TA Lister and D Bonnet. (2005). Characterization of cells with a high aldehyde dehydrogenase activity from cord blood and acute myeloid leukemia samples. *Stem Cells* 23:752–760.
- Marcato P, CA Dean, CA Giacomantonio and PW Lee. (2011). Aldehyde dehydrogenase: its role as a cancer stem cell marker comes down to the specific isoform. *Cell Cycle* 10:1378–1384.
- Patel M, L Lu, DS Zander, L Sreerama, D Coco and JS Moreb. (2008). ALDH1A1 and ALDH3A1 expression in lung cancers: correlation with histologic type and potential precursors. *Lung Cancer* 59:340–349.
- Sullivan JP, M Spinola, M Dodge, MG Raso, C Behrens, B Gao, K Schuster, C Shao, JE Larsen, et al. (2010). Aldehyde dehydrogenase activity selects for lung adenocarcinoma stem cells dependent on notch signaling. *Cancer Res* 70:9937–9948.
- Yoshida A, A Rzhetsky, LC Hsu and C Chang. (1998). Human aldehyde dehydrogenase gene family. *Eur J Biochem* 251:549–557.
- Sophos NA and V Vasiliou. (2003). Aldehyde dehydrogenase gene superfamily: the 2002 update. *Chem Biol Interact* 143–144:5–22.
- Vasiliou V and DW Nebert. (2005). Analysis and update of the human aldehyde dehydrogenase (ALDH) gene family. *Hum Genomics* 2:138–143.
- O'Brien PJ, AG Siraki and N Shangari. (2005). Aldehyde sources, metabolism, molecular toxicity mechanisms, and possible effects on human health. *Crit Rev Toxicol* 35:609–662.
- You Y, EJ Richer, T Huang and SL Brody. (2002). Growth and differentiation of mouse tracheal epithelial cells: selection of a proliferative population. *Am J Physiol Lung Cell Mol Physiol* 283:L1315–L1321.
- Trapnell C, L Pachter and SL Salzberg. (2009). TopHat: discovering splice junctions with RNA-Seq. *Bioinformatics* 25:1105–1111.
- Trapnell C, BA Williams, G Pertea, A Mortazavi, G Kwan, MJ van Baren, SL Salzberg, BJ Wold and L Pachter. (2010). Transcript assembly and quantification by RNA-Seq reveals

- unannotated transcripts and isoform switching during cell differentiation. *Nat Biotechnol* 28:511–515.
21. Anders S and W Huber. (2010). Differential expression analysis for sequence count data. *Genome Biol* 11:R106.
 22. Feige JN, M Lagouge, C Canto, A Strehle, SM Houten, JC Milne, PD Lambert, C Matakai, PJ Elliott and J Auwerx. (2008). Specific SIRT1 activation mimics low energy levels and protects against diet-induced metabolic disorders by enhancing fat oxidation. *Cell Metab* 8:347–358.
 23. Cicalese A, G Bonizzi, CE Pasi, M Faretta, S Ronzoni, B Giulini, C Brisken, S Minucci, PP Di Fiore and PG Pelicci. (2009). The tumor suppressor p53 regulates polarity of self-renewing divisions in mammary stem cells. *Cell* 138:1083–1095.
 24. Alnouti Y and CD Klaassen. (2008). Tissue distribution, ontogeny, and regulation of aldehyde dehydrogenase (Aldh) enzymes mRNA by prototypical microsomal enzyme inducers in mice. *Toxicol Sci* 101:51–64.
 25. Keung WM and BL Vallee. (1993). Daidzin: a potent, selective inhibitor of human mitochondrial aldehyde dehydrogenase. *Proc Natl Acad Sci U S A* 90:1247–1251.
 26. Ren S, TF Kalthorn and JT Slattery. (1999). Inhibition of human aldehyde dehydrogenase 1 by the 4-hydroxycyclophosphamide degradation product acrolein. *Drug Metab Dispos* 27:133–137.
 27. Canuto RA, M Maggiora, A Trombetta, G Martinasso and G Muzio. (2003). Aldehyde dehydrogenase 3 expression is decreased by clofibrate via PPAR gamma induction in JM2 rat hepatoma cell line. *Chem Biol Interact* 143–144:29–35.
 28. Tsao PN, M Vasconcelos, KI Izvolsky, J Qian, J Lu and WV Cardoso. (2009). Notch signaling controls the balance of ciliated and secretory cell fates in developing airways. *Development* 136:2297–2307.
 29. Guseh JS, SA Bores, BZ Stanger, Q Zhou, WJ Anderson, DA Melton and J Rajagopal. (2009). Notch signaling promotes airway mucous metaplasia and inhibits alveolar development. *Development* 136:1751–1759.
 30. Banh A, N Xiao, H Cao, CH Chen, P Kuo, T Krakow, B Bavan, B Khong, M Yao, et al. (2011). A novel aldehyde dehydrogenase-3 activator leads to adult salivary stem cell enrichment *in vivo*. *Clin Cancer Res* 17:7265–7272.
 31. Khanna M, CH Chen, A Kimble-Hill, B Parajuli, S Perez-Miller, S Baskaran, J Kim, K Dria, V Vasiliou, D Mochly-Rosen and TD Hurley. (2011). Discovery of a novel class of covalent inhibitor for aldehyde dehydrogenases. *J Biol Chem* 286:43486–43494.
 32. Moreb JS, D Ucar, S Han, JK Amory, AS Goldstein, B Ostmark and LJ Chang. (2012). The enzymatic activity of human aldehyde dehydrogenases 1A2 and 2 (ALDH1A2 and ALDH2) is detected by Aldefluor, inhibited by diethylaminobenzaldehyde and has significant effects on cell proliferation and drug resistance. *Chem Biol Interact* 195:52–60.
 33. Katada C, M Muto, M Nakayama, S Tanabe, K Higuchi, T Sasaki, M Azuma, K Ishido, N Katada, et al. (2012). Risk of superficial squamous cell carcinoma developing in the head and neck region in patients with esophageal squamous cell carcinoma. *Laryngoscope* 122:1291–1296.
 34. Oyama T, H Nagayoshi, T Matsuda, M Oka, T Isse, HS Yu, TT Pham, M Tanaka, N Kagawa, K Kaneko and T Kawamoto. (2010). Effects of acetaldehyde inhalation in mitochondrial aldehyde dehydrogenase deficient mice (Aldh2-/-). *Front Biosci* 2:1344–1354.
 35. Park JY, K Matsuo, T Suzuki, H Ito, S Hosono, T Kawase, M Watanabe, I Oze, T Hida, et al. (2010). Impact of smoking on lung cancer risk is stronger in those with the homozygous aldehyde dehydrogenase 2 null allele in a Japanese population. *Carcinogenesis* 31:660–665.
 36. Lewis SJ and GD Smith. (2005). Alcohol, ALDH2, and esophageal cancer: a meta-analysis which illustrates the potentials and limitations of a Mendelian randomization approach. *Cancer Epidemiol Biomarkers Prev* 14:1967–1971.
 37. Matsuo K, I Oze, S Hosono, H Ito, M Watanabe, K Ishioka, S Ito, M Tajika, Y Yatabe, et al. (2013). The aldehyde dehydrogenase 2 (ALDH2) Glu504Lys polymorphism interacts with alcohol drinking in the risk of stomach cancer. *Carcinogenesis* 34:1510–1515.
 38. Balber AE. (2011). Concise review: aldehyde dehydrogenase bright stem and progenitor cell populations from normal tissues: characteristics, activities, and emerging uses in regenerative medicine. *Stem Cells* 29:570–575.
 39. Sato T, JH van Es, HJ Snippert, DE Stange, RG Vries, M van den Born, N Barker, NF Shroyer, M van de Wetering and H Clevers. (2011). Paneth cells constitute the niche for Lgr5 stem cells in intestinal crypts. *Nature* 469:415–418.
 40. Cummings BS, J McHowat and RG Schnellmann. (2000). Phospholipase A(2)s in cell injury and death. *J Pharmacol Exp Ther* 294:793–799.
 41. Suraneni MV, R Schneider-Broussard, JR Moore, TC Davis, CJ Maldonado, H Li, RA Newman, D Kusewitt, J Hu, P Yang and DG Tang. (2010). Transgenic expression of 15-lipoxygenase 2 (15-LOX2) in mouse prostate leads to hyperplasia and cell senescence. *Oncogene* 29:4261–4275.
 42. Kenchegowda S, NG Bazan and HE Bazan. (2011). EGF stimulates lipoxin A4 synthesis and modulates repair in corneal epithelial cells through ERK and p38 activation. *Invest Ophthalmol Vis Sci* 52:2240–2249.
 43. Andersson CK, HE Claesson, K Rydell-Tormanen, S Swedmark, A Hallgren and JS Erjefalt. (2008). Mice lacking 12/15-lipoxygenase have attenuated airway allergic inflammation and remodeling. *Am J Respir Cell Mol Biol* 39:648–656.

Address correspondence to:

Dr. Brigitte N. Gomperts
 Department of Pediatrics
 Children's Discovery and Innovation Institute
 David Geffen School of Medicine at UCLA
 Mattel Children's Hospital
 10833 Le Conte Avenue, A2-410MDCC
 Los Angeles, CA 90095

E-mail: bgomperts@mednet.ucla.edu

Received for publication July 4, 2013

Accepted after revision October 30, 2013

Prepublished on Liebert Instant Online October 30, 2013